Progress Report

INVESTIGATION OF DEEP LEVEL DEFECTS IN EPITAXIAL SEMICONDUCTING ZINC SULPHO-SELENIDE

B. W. Wessels

Northwestern University
Evanston, Illinois 60201

February 15, 1981

Report for the Period 6/15/80 - 6/14/81

Prepared for the Department of Energy under
Contract No. DE-AS02-79ER10390

NOTICE

DISCLAIMER

ABSTRACT

High conductivity ZnSe single crystalline films have been heteroepitaxially deposited on GaAs substrates using open tube chemical vapor transport. Unintentionally doped films had net donor densities of 10^{14} - 10^{16} cm^{-3} and resistivities of 1 to 10^{3} ohm cm. Resistivity was found to be strongly dependent upon zinc partial pressure during deposition. Electron mobilities of the order of 50-200 cm^{2}/V sec were observed which suggested that the films are highly compensated. Properties of the deep level defects in heteroepitaxially grown ZnSe have been investigated using transient capacitance spectroscopy. A series of electron traps were observed with activation energies of 0.33, 0.35, 0.42 0.71 and 0.86 eV in Au/ZnSe Schottky diodes. Trap concentration ranged from 10^{12} to 10^{14} cm^{-3} and depended on the zinc partial pressure. A model for the defect structure of ZnSe was proposed. Growth studies of ZnS_xSe_{1-x} on GaAs were begun.

PROGRESS REPORT

This report describes the research on electronically active defects in semiconducting zinc sulfoselenide for the period June 15, 1980 - Feb. 15, 1981. Research was performed in three main areas including preparation and electronic doping of heteroepitaxial zinc sulfoselenide, electrical characterization of the thin film material using Hall effect measurements and the transient capacitance spectroscopy of deep level defect states in the as-grown material.

HIGH CONDUCTIVITY HETEROEPITAXIAL ZnSe FILMS

Although low resistivity bulk ZnSe has been prepared by the Zn anneal technique[1], homogeneous, low resistivity thin films have been extremely difficult to prepare. To date, beside this study, there has been only one report of high conductivity as-grown ZnSe epitaxial layers[2]. In that particular case the high conductivity ZnSe was prepared by molecular beam epitaxy. The reason for the difficulty in preparing high conductivity ZnSe is not well understood and is the subject of considerable controversy. Two proposed theories are that high resistivity occurs either as a result of self-compensation by native defects or by compensation by residual impurities. Nevertheless, in this study we have recently reported high conductivity as-grown ZnSe films with resistivities as low as 0.4 ohm-cm have been prepared without intentional doping.

ZnSe layers were grown by open tube chemical vapor transport on polished (100) GaAs n-type and p-type substrates, which were chemically etched in 5:5:1 H_2SO_4: H_2O: H_2O_2 before deposition. The source for deposition consisted of electronic grade ZnSe. In addition, in order to grow films under an excess zinc pressure, a separate zinc source was incorporated into the growth system and heated to 300-600°C. Palladium diffused hydrogen served as the carrier gas for the transport reaction. For a ZnSe source temperature of 1000°C, a substrate temperature of 750°C and H_2 flow rate of 500 cc/min., a growth rate of 0.3 μ/min. was observed. Typical layer thicknesses were 5-30 μm.

The surface morphology of the as-grown ZnSe was investigated using a scanning electron microscope (SEM) and Normarski contrast microscope. Scanning electron microscopy indicated a smooth featureless morphology at 200X, as

shown in Fig. (1). However, a slight surface texture was observed at 5000X. Channeling patterns were observed in the SEM on the heteroepitaxial ZnSe, which indicates the layers were single crystalline. Scanning Auger microscopic analysis using the PHI 590A system on cleaved layers revealed that the material was ZnSe and that no appreciable interdiffusion at the substrate-layer interface occurred. The composition transition region between the ZnSe-GaAs was determined to be less than 0.5μ, which is the limit of resolution of the instrument.

Net donor concentrations for the as-grown layers were determined from capacitance-voltage measurements on gold Schottky barriers 0.8 mm^2 in area. Ohmic contacts to the n^+ GaAs substrates were indium dots that were alloyed at 250°C in a nitrogen atmosphere. The n^+ GaAs served as an ohmic contact to the n-type ZnSe. Donor densities of the as-grown layers varied between 1×10^{14} cm^{-3} and 2×10^{16} cm^{-3} as reported in Table 1. The built-in voltages of the Schottky barriers were typically 1.2 - 1.9 V, which is good agreement with built-in voltages previously reported[3]. Although in some cases, larger apparent built-in voltages were observed, which could be attributed to the presence of a thin (≤ 100 Å) interfacial insulating layer with either interface states in equilibrium with the metal or a net charge at the insulator-semiconductor interface[4].

In Fig. (2) the resistivity of the as-grown ZnSe deposited on p-type GaAs is reported as a function of zinc/selenium ratio present during deposition. For ZnSe grown at 725°C without excess zinc added to the growth system, resistivities of the order of 5×10^3 Ωcm or greater were observed which is consistent with past observations[5]. However films grown under

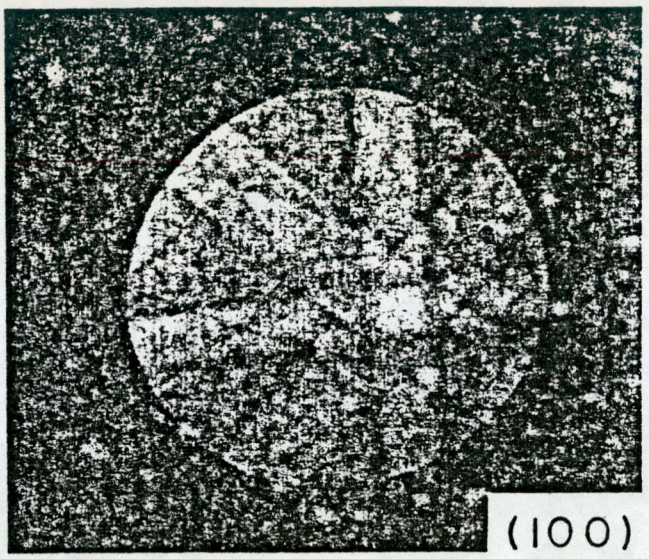

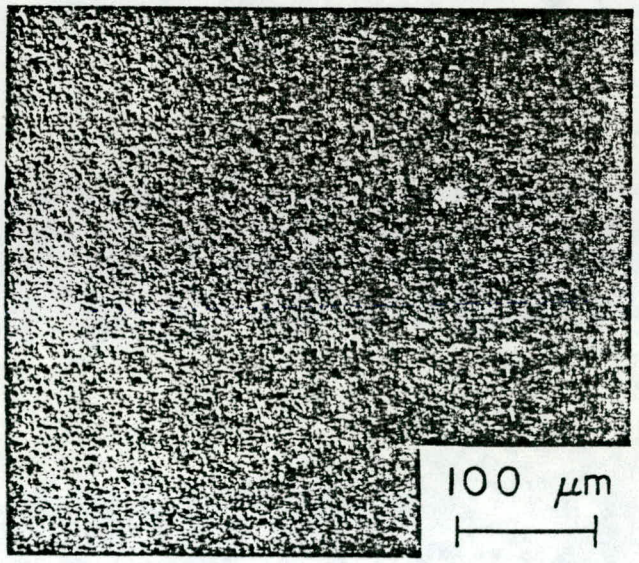

Fig.(1) (a) SEM channeling pattern of heteroepitaxial ZnSe (b) Surface morphology

Table 1 Net donor densities in heteroepitaxial ZnSe

Sample No.	N_D-N_A (cm^{-3})	V_{bi} (Volts)	Zinc over pressure (10^{-3}atm)	Thickness (μm)
111	1×10^{14}	1.20	0	18.0
112	4×10^{14}	1.90	5	11.3
114	5×10^{14}	1.40	12.6	4.0
116	1×10^{15}	1.75	14.5	4.0
157	1×10^{16}	3.10	24.1	2.4
160	2×10^{16}	2.70	34.9	6.5

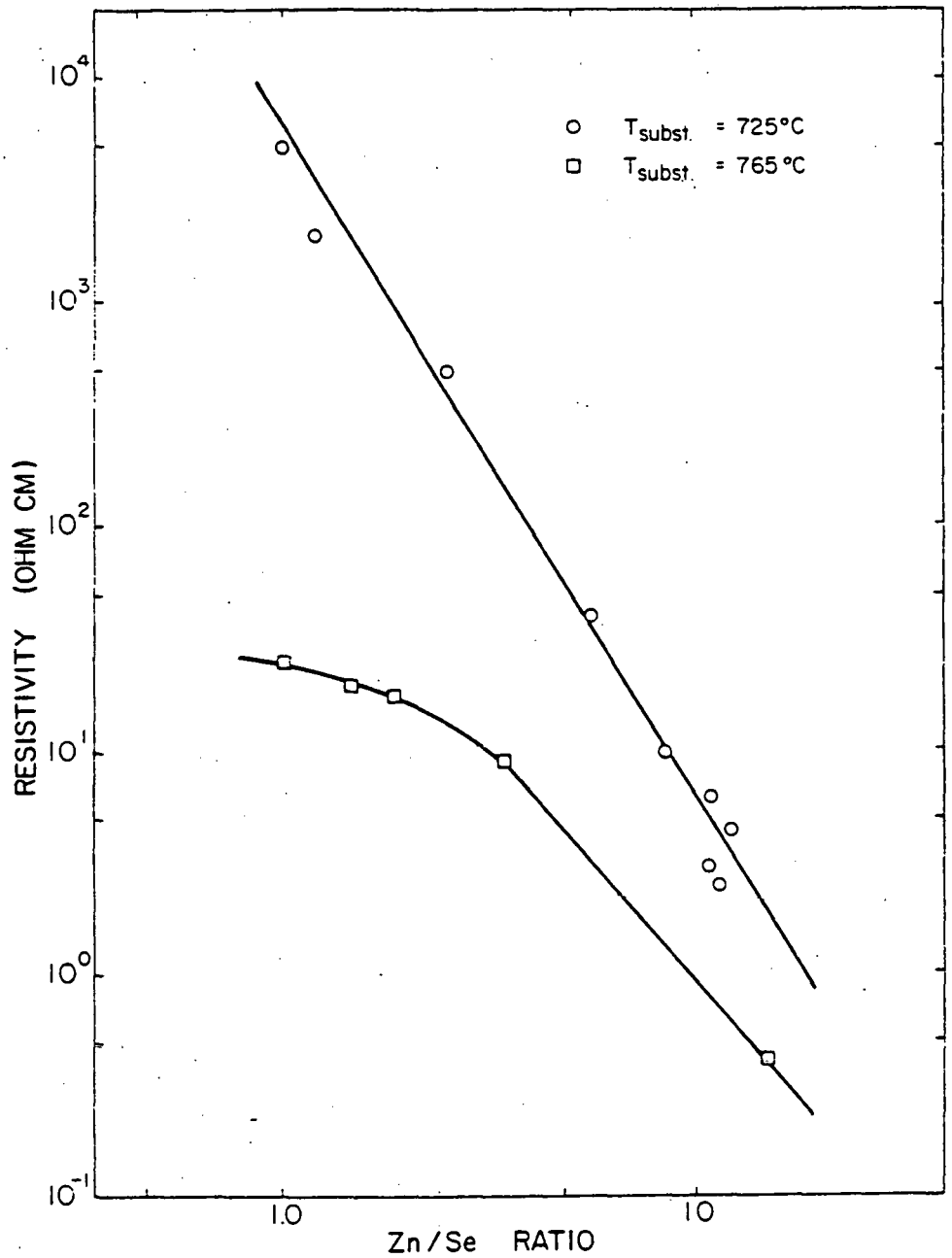

Fig. (2) Resistivity of ZnSe as a function of Zn/Se ratio

excess zinc conditions showed a marked decrease in film resistivy to 2.0 Ωcm. Presumably the excess zinc reduces the compensation of residual donors by native acceptors such as the doubly ionized zinc vacancy, as will be discussed in a later section. The residual donor impurity responsible for the high conductivity of the layers has not yet been identified, though one possible impurity could be gallium which has diffused from the GaAs substrate. Gallium has been previously reported as a shallow donor in ZnSe with an ionization energy of 28 meV[6]. Moreover gallium has been found to be the major contaminant in heteroepitaxial CdS[7] and CdZnS[8] grown on GaAs at high substrate temperatures. The fact that in this study the resistivity decreases with higher substrate temperature further substantiates Ga being the major dopant.

In regard to the previous difficulty in obtaining low resistivity ZnSe thin films, we believe that extrinsic impurities play an important role in determining the resistivity of the as-grown layers. These extrinsic impurities are both a source of shallow and deep states that serve to compensate the semiconductor. Nevertheless, once these extrinsic defect centers are eliminated by careful crystal growth techniques, intrinsic defects such as vacancies, and interstitials, could control the resistivity, as evidenced by the zinc pressure dependence of the resistivity, Doping of the ZnSe was attempted by incorporating a metallic source into the growth apparatus in the high temperature region. Group III elements were explored including aluminum, gallium, and indium. Because of the relative low vapor pressures of aluminum and gallium, only indium appeared to dope the films. Even when indium doped, however, it was noted that films grown under stoichiometric conditions had high resistivities of the order of 10^4-10^5 ohm cm. Nevertheless when excess zinc was added to the system, low resistivity material of the order of 1-10 ohm-cm could be readily obtained.

PREPARATION OF THIN FILM ZnSSe

ZnS_xSe_{1-x} epitaxial layers were grown by the same hydrogen transport technique used in the preparation of ZnSe. Palladium diffused H_2 was passed over a high purity ZnSe source. A separate H_2S gas source served as the sulfur supply. The H_2 flow over the ZnSe source was 500 cm^3/min. Two different electronic grade H_2S sources were used. One contained 15% H_2S in H_2(Synthatron Corp.), the other 1% H_2S in H_2. With the tank containing 15% H_2S, H_2S flow rates could be varied from 1 cm^3/min. to 4 cm^3/min. This corresponded to sulfur fraction of x = .15 to .50 in the ZnS_xSe_{1-x} film, as determined by lattice-parameter measurements. A tank containing 1% H_2S was used to obtain flowrates between 0.22 and 1.5 cm^3/min. Lower flow rates should be possible using this tank, to about 0.12 cm^3/min. H_2S. This would correspond to x = .02 for S in the thin film. For our studies, total group VI/VII ratios in the gas phase varied from 2 to 4 in the crystal growth runs. All ZnSSe crystals were grown on (100) GaAs substrates at substrate temperatures between 740°C and 780°C.

The samples were grown for one hour which resulted in an epitaxial growth layer of approximately 6 μm thick. This thickness is precisely what is needed for x-ray diffraction analysis. If thicker layers such as 10 μm are used, absorption in the ZnSe layer is too high in order to make proper identification of the GaAs x-ray diffraction peaks.

Good growth morphology was observed for most of the crystals grown under these conditions. Zinc sulfoselenide layers were mirror smooth and revealed few flaws under microscopic examination. However some samples showed small hillocks, approximately 3 μm in diameter. These hillocks disappeared with improved substrate etching techniques. In some films a cross hatched pattern

was sometimes observed under high magnification (500X). This pattern was attributed to cracks in the film as a result of the ZnS_xSe_{1-x} film having a smaller lattice parameter than the GaAs substrate. These lines were more abundant with ZnS_xSe_{1-x} having a higher value of x e.g. x = 0.15 which corresponds to a lattice constant mismatch of 1.7%. These lines disappeared in samples having sulfur content closer to x = .05.

In some cases these lines would terminate near a yellow area on the edge of the sample, in a region thought to be polycrystalline. These yellowish areas were particularly abundant in the earlier runs, each patch consisting of a long stripe running the length of the sample. These areas flaked off when the sample was subsequently cleaned, suggesting poor epitaxy. This material was thought to be sulfur rich. Consequently the amount of H_2S produced crystals without yellowish areas.

In the initial runs, ZnSe was grown first for approximately 15 minutes, before ZnS_xSe_{1-x} was grown for 1 hour to provide a single step graded layer. This practice of growing a middle layer of ZnSe was later found to be unnecessary for layers with small sulfur concentrations and was later abandoned.

Sulfur content was determined with x-ray diffraction using Vegard's law. ZnSe has a slightly larger lattice parameter than GaAs. For ZnS_xSe_{1-x} having x = 0.0546, there exists theoretically a perfect lattice match between layer and substrate. Samples have been grown having sulfur content of $x = 0.055 \pm .001$ in which no distinct ZnS_xSe_{1-x} x-ray peak could be observed from the GaAs peak using the (400) reflection.

X-ray diffraction scans were performed on all samples grown at various H_2S flow rates to determine lattice parameter and insure crystallity of epitaxial layers. Large angle diffractometer scans on each sample proved

that all crystals were single crystals. Sulfur content was then determined using a high resolution scan of the (400) peak. The GaAs peak obtained was first corrected to the true zero, then the ZnS_xSe_{1-x} peak was corrected similarly. The percent sulfur concentration was calculated from the difference of the d_{400} spacing

$$\frac{d_{ZnSSe} - d_{ZnSe}}{d_{ZnSe} - d_{ZnS}} \times 100 = \%S \qquad (1)$$

where $d_{ZnSSe} - d_{ZnSe}$ and d_{ZnS} are the "d" spacings for ZnSSe (as measured), ZnSe and ZnS, respectfully: d_{ZnSe} and d_{ZnS} were determined from powder diffraction x-ray films to be

$$d_{ZnSe} - d_{ZnS} = 0.0650 \text{ Å}$$

It should be noted however, some ZnS_xSe_{1-x} diffraction peaks are observed to be slightly asymmetric. This could be due to an inhomogeneous concentration of sulfur between the interface and the surface of the layer.

Table 2 shows H_2S flow rate and % sulfur measured for various samples. As observed from Table 2, good control of sulfur content can be achieved through variation of flow rates. Samples of ZnS_xSe_{1-x} can be grown up to sulfur contents of 20% using the tank of 1% H_2S in hydrogen.

Resistivity of the as grown zinc sulfoselenide is greater than 10^4 ohm-cm. This is to be expected since the material is being prepared under group VI excess partial pressures. Experiments are under way to prepare thin films under zinc rich conditions to ascertain whether low reisitivity thin films can be obtained.

Table 2 Composition of ZnS_xSe_{1-x} as a function of H_2S flow rate

Sample #	H_2S cc/min.	S(layer)%	S/Se (gas phase)
S-14	0.22	5.5 $\pm$ .05	0.20
S-13	0.36	7.2	0.33
S-11	0.63	14.7	0.64
S-5	1.0	15.6	0.81
S-12	1.1	17.0	1.0
S-9	4	47.7	3.0

HALL EFFECT MEASUREMENTS

In an effort to understand the doping compensation mechanisms of the ZnSe thin films, the electronic properties were studied using the Hall effect measurements. From the temperature dependence of the carrier concentration and the Hall mobility, the donor and acceptor concentrations as well as the compensation ratios of the thin films were determined.

Hall mobility measurements were performed on heteroepitaxial ZnSe layers that were deposited on p-type GaAs substrates having net acceptor concentration of 2×10^{17} cm^{-3}. P-type GaAs substrates were extensively used since it was observed that Cr doped GaAs went n-type during processing. This would lead to anomalously low resistivity values. Ohmic contacts to the ZnSe layers were formed by alloying indium onto the samples at $300^{o}C$ under an inert Ar sample. Resistivities and Hall constants were measured using van der Pauw technique on samples approximately 8x8 mm^2 in area. Samples were mounted on an insulated holder and care was taken to minimize any leakage currents arising from shunting by the p-type GaAs substrate by using small measurement currents. For the van der Pauw measurements, an applied magnetic field of 4.5 kilogauss was used. Measurements were performed over a temperature range of 77 to 300 K.

The carrier concentration n and the Hall mobility μ were calculated from the equations:

$$n = r/eR \qquad (2)$$

$$\mu = R/\rho \qquad (3)$$

where R equals the Hall constant and ρ the resistivity. A value of 1.0 was assumed for the Hall factor r.

The Hall measurememt results for seven undoped n-type ZnSe films deposited on p-type GaAs are reported in Table 3. The room temperature electron concentrations were in the range of 1×10^{13} cm^{-3} to 2.0×10^{16} cm^{-3} depending upon substrate temperature and ZnSe ratio used during growth. In general, high electron concentrations were observed for materials grown at substrate temperatures of 760°C and Zn/Se ratios of greater than one.

Table 4 reports the electrical properties of samples that were deliberately indium doped during vapor growth. For these samples, the electron concentrations at room temperature were in the range of $1 - 10 \times 10^{16}$ cm^{-3}. The upper limit is a factor of 5 greater than what is observed in the undoped samples. The electron concentration appeared to be relatively insensitive to substrate temperature. Moreover the electron concentration was only weakly dependent on Zn/Se ratio. It is observed that the carrier concentration varies as $(Zn/Se)^{\frac{1}{2}}$ for the indium doped films. The temperature dependence of carrier concentration, n was analyzed using the single valley model[9]:

$$\frac{n\ (n + N_A)}{N_D - N_A - n} = \frac{2(2\Pi m^* kT)^{3/2}}{gh^3} \exp -E_d/kT \qquad (4)$$

where N_D and N_A are the concentrationsof the donors and acceptor, respectively, E_d is the ionization energy of the donors, g is the spin degeneracy which is taken to be 2 and m^* the density of states effective mass for electrons was taken as 0.16 m. In Eq. 2 the adjustable parameters are N_D,N_A and E_d. The results of the analysis are given in Table 5. It should be noted that n vs. 1/T curves could only be fitted over a limited temperature range since the

Table 3 Electrical Properties of undoped n-type ZnSe

Film No.	Code No.	Thickness	Zn/Se ratio	Growth T(°C)	n cm^{-3}	μ
1	150	4.2	1.1	717	1×10^{13}	10
2	152	6.4	2.0	725	6×10^{14}	36
3	153	10	4.1	757	2.5×10^{14}	85
4	155	18	1.1	760	7.0×10^{15}	125
5	156	16	1.3	755	7.0×10^{15}	120
6	157	2.5	13	757	7.0×10^{16}	87
7	158	2.5	1.1	762	2.0×10^{16}	200

Table 4 Electrical Properties of indium doped n-type ZnSe

Film No.	Code No.	Thickness μm	Zn/Se ratio	Growth T(°C)	n cm^{-3} x 10^{16} 296 K	μ cm^2/V sec
1	195	10	2.3	765	10.0	74
2	200	10	5.6	770	6.6	106
3	201	10	3.3	772	3.4	130
4	202	11	1.5	775	2.9	97
5	203	11	1.01	777	1.0	52
6	207	6	2.4	737	4.0	67
7	210	5	9.6	732	7.0	82

onset of impurity band conduction was observed a low temperatures[9]. In analyzing the temperature dependence data, it was assumed that $N_A > n$, which is consistent with the Hall mobility measurements. For these conditions Eq. 4 can be simplified to:

$$N \simeq \frac{N_c}{g} \left[(N_D - N_A)/N_A\right] e^{-E_d/kT} \qquad (5)$$

As is evident in Table 5, the compensation of the semiconductors is high with compensation of 99% being observed in sample 158. Except for sample 158, the calculated donor ionization energy was zero, indicating that the donor density is indeed greater than 3×10^{17} cm^{-3} in the thin films.

From the temperature dependence of the mobility, the number of ionized acceptors were determined by measuring the contribution of ionized impurities to the scattering of carriers[10]. This contribution was obtained from the total mobility by assuming no correlation among scattering processes. Consequently, the total mobility is given by

$$\frac{1}{\mu} = \lesssim \frac{1}{\mu_i} \qquad (6)$$

For the ZnSe films it was assumed that only ionized impurity scattering μ_I and polar optical scattering μ_{po} are important in the temperature range of interest as was done in the work of Jones and Woods on bulk ZnSe[11]. The mobility when limited by polar optical scattering is given by:

$$\mu_{po} = A\, T^{\frac{1}{2}} \left(\exp^{\theta/T} - 1\right) G \qquad (7)$$

where A is empirically determined from the data of Aven [12] and θ is the equivalent temperature for the characteristic longitudinal optical vibration. For ZnSe, θ is equal to 364K[11]. G is a slightly varying function of temperature and effective mass of the order of unity.

For scattering by ionized impurities, the mobility is given by the Brooks-Herring formula[10]:

$$\mu_I = \frac{3.28\times10^{15}\ T^{3/2}}{N_I}\,\epsilon_o\left(\frac{m}{m^*}\right)^{\frac{1}{2}} \qquad x\left\{\ln\ 1.29\times10^{14}\,(m^*/m)\ \epsilon_o\,\frac{T}{n'}\right\}^{-1} \qquad (8)$$

where the ionized concentration $N_I = n + 2\ N_A$, ϵ_o is the relative dielectric constant taken as 9.1 for ZnSe and $n' = n + \frac{(n + N_A)\ (N_D - N_A - n)}{N}$ (9)

The term n' can be simplified by noting that at 300K, $n \cong N_D - N_A$, therefore $n' = n$. For the thin films, the highest mobility observed was 210 cm^2/V sec. Since the measured value of the mobility for ZnSe is considerably below the value for mobility limited by polar optical scattering 530 cm^2/V sec. at room temperature, the dominant scattering mechanism is presumably ionized impurity scattering in the thin film material. At temperatures below 120 K, however, the mobility is limited by impurity band conduction, which is consistent with the finding of Sethi and Mathur[9] on bulk ZnSe crystals. Using Eq. (8) the acceptor concentration N_A was determined as reported in Table 6. The acceptor concentrations were of the order of 10^{18} cm^{-3} indicating that the ZnSe films are strongly compensated. Addition of indium tends to lessen the compensation, which is consistent with indium acting as a simple donor. The nature of the compensating defects is presently under investigation.

Table 5 Electronic Properties of thin film ZnSe

Sample	n_{300K} 10^{16} (cm^{-3})	E_d meV	N_A/N_D	Zn/Se	In/Zn
200	6.6	0	-	5.6	0.01
207	3.6	0	-	2.4	0.01
203	1.0	0	-	1.01	0.02
195	11	0	-	2.3	0.12
158	1.5	23	.99	1.1	0
W-1	1.3	0	-	4.8	0
W-3	1.5	0	-	4.6	0

Table 6 Acceptor concentration in n-type ZnSe

Sample	μ_{300K} ($cm^2/Vsec$)	n_{300K} $10^{16}(cm^{-3})$	N_A 10^{18} (cm^{-3})	$\frac{N_A}{N_D}$ [a]
200[b]	106	6.6	2.4	.97
207[b]	73	3.6	3.4	.99
203[b]	52	1.0	4.2	.997
195[b]	78	11	3.9	.97
158	199	1.5	0.79	.98
W-1	104	1.3	1.9	.99
W-3	95	1.5	2.2	.99

a - calculated assuming $n_{300K} = N_D - N_A$

b - indium doped

DEEP LEVEL DEFECT STUDIES

To determine the nature of the grown-in defects in ZnSSe defects were detected by using transient capacitance spectroscopy on gold Schottky diodes. Although this technique has been mainly used to study silicon and III-V compounds[13], recently its use has been extended to studied of II-VI compounds, showing its applicability for investigating defects in large band-gap semiconductors. The technique consists of periodically reducing the bias of a junction from its quiescent reverse bias state. The capacitance transients, which result from thermal emission of trapped carriers, are then monitored via a differential capacitance meter and a boxcar averager as a function of temperature. Capacitance time constants of the order of 10 micro-seconds to 10 milliseconds are readily measured with a 20 MHz drive frequency. During this contract period both ZnSe heterojunctions and Schottky barriers were characterized using capacitance spectroscopy. Fig. 3 shows a typical transient capacitance spectrum for Au/ZnSe Schottky barrier in undoped material. The spectrum reveals four well resolved peaks indicative of discrete trapping states. Fig. 4 gives the measured thermal emission rates as a function of the reciprocal temperature for the traps observed in several samples. From the detailed balance equation

$$e_n = \tau^{-1} = N_c \langle v \rangle \sigma_\infty \exp(\alpha/k) \exp(-E_t kT) \qquad (10)$$

where e_n is the emission rate, N_c is the density of states and $\langle v \rangle$ the thermal velocity, we obtained the trap energy E_t and the approximate value of the capture cross section; σ_∞ is the temperature independent prefactor of the capture cross section and α is the temperature coefficient of the trap depth. In calculating the trap energy and crosssection, a least square analysis was used

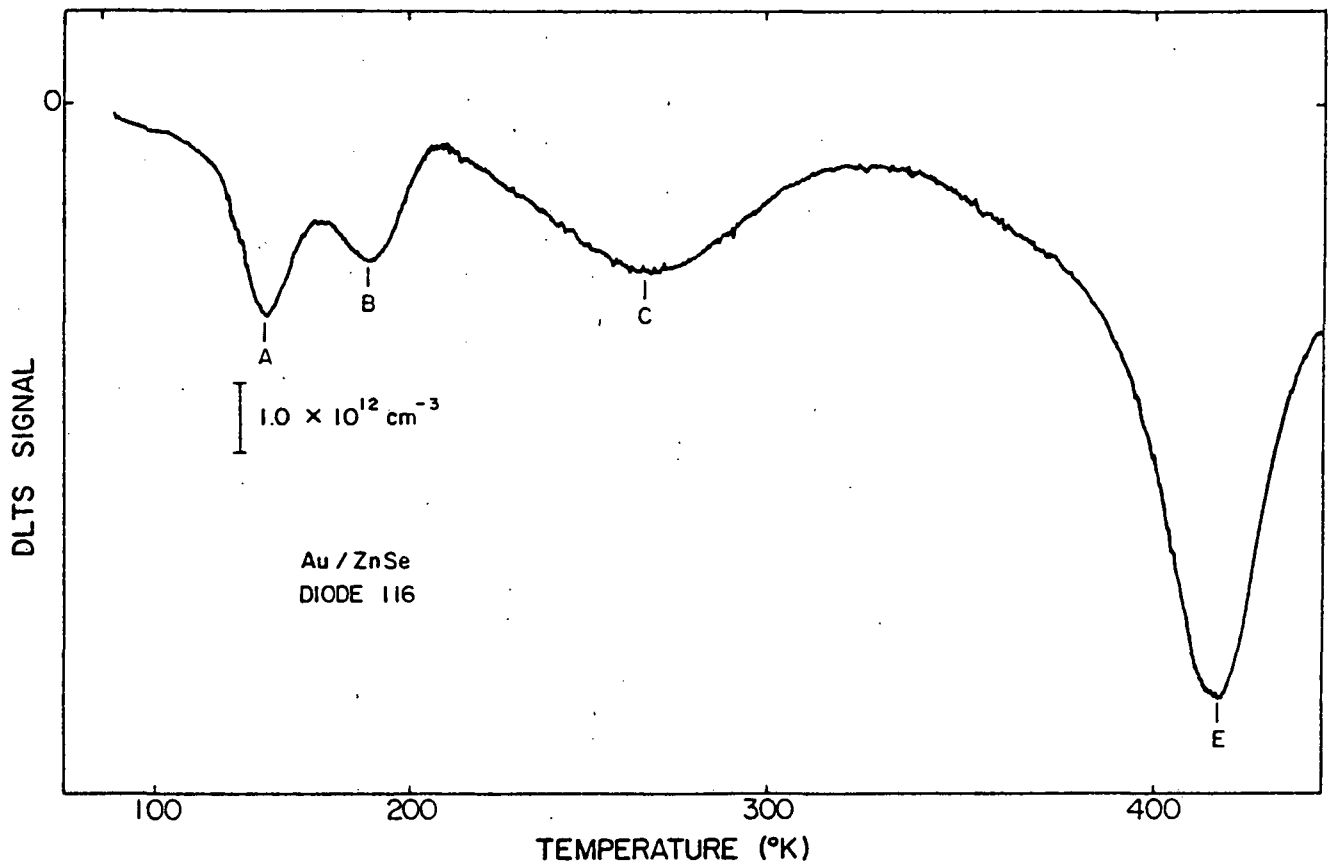

Fig. (3) DLTS spectrum for Au/ZnSe Schottky diode

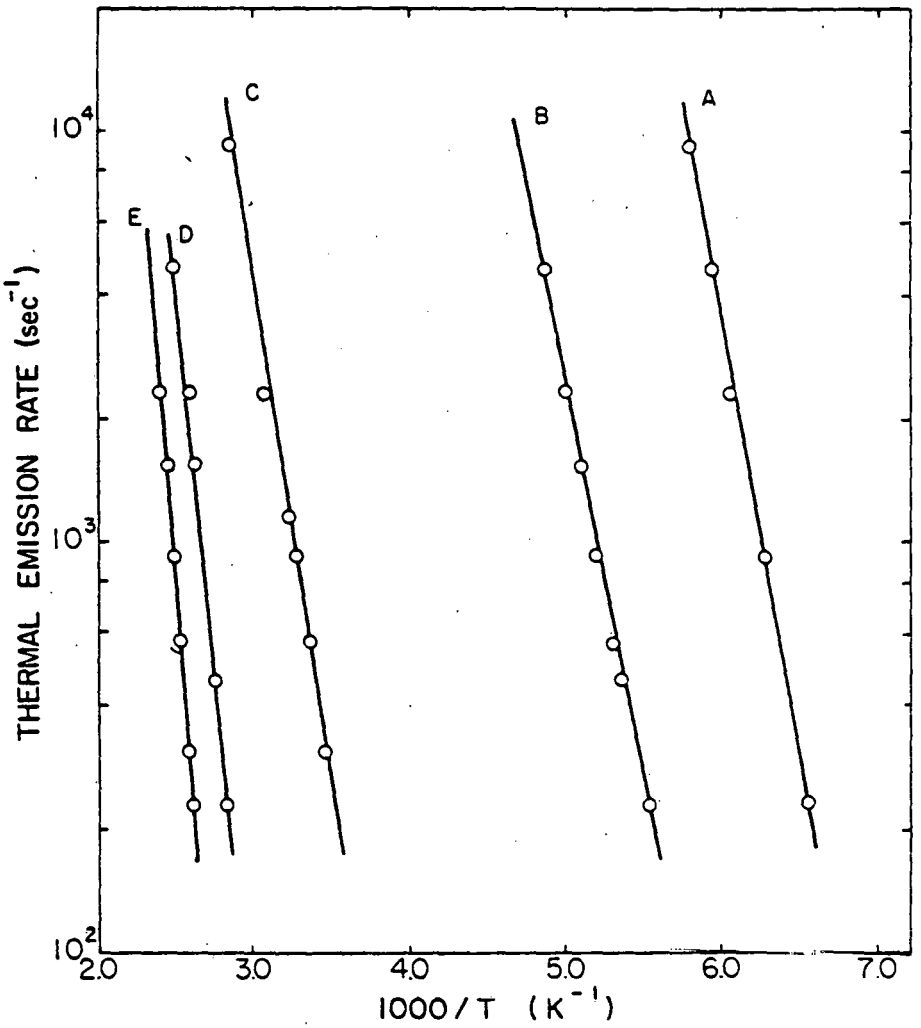

Fig. (4) Emission rate vs. 1/T K^{-1} for Au/ZnSe

Table 7 Experimentally determined trap parameters in ZnSe/GaAs diodes

Trap	ΔE_t (eV)	$\sigma_\infty \exp \alpha/k$ (cm^2)	T range (K)
I	0.15	-	100 - 120
A	0.33	1×10^{-13}	155 - 180
B	0.35	2×10^{-14}	185 - 215
G	0.54	3×10^{-14}	230 - 310

taking into account the T^2 dependence of $N_c \langle v \rangle$. The values obtained for each trap observed are reported in Table 8. Traps (A,B,C,E) were routinely observed in the as-grown ZnSe. The concentrations of electron traps were in the range of 10^{12} - 10^{14} cm^{-3}. The sensitivity of defect detection was 3×10^{11} defects/cm^3. It should be noted that the measured value of the capture cross section prefactor varied over an order of magnitude from sample to sample, and the average value is given in Table 8. A similar behavior was reported in Cu/CdS polycrystalline[14] and single crystalline diodes[15]. Therefore to precisely measure the capture cross-sections of the traps, a more direct method was subsequently used. This technique involves measuring the magnitude of the transient capacitance signal as a function of majority carrier pulse width. The quantity of $\Delta C_\infty - \Delta C$ is plotted as a function of pulse width t where ΔC is the transient capacitance observed for a pulse length t_p. The observed capture time τ_c is related to the capture cross-section according to the following equation:

$$\tau_c^{-1} = \sigma_n \langle v \rangle n \qquad (11)$$

Using this technique, the capture cross-section was measured for three traps I, A and E in Au/ZnSe Schottky diodes. For a measured capture time of 13 μsec, $n = 5 \times 10^{16}$ cm^{-3} and $\langle v \rangle = 7.7 \times 10^6 cm^{-1}$/sec. at 154 K a value of $2 \times 10^{-19} cm^2$ is obtained for the capture cross-section of trap A. Similarly, values of $\sigma_n = 9.4 \times 10^{-19}$ cm^2 and $\tau_n = 4.4 \times 10^{-19}$ cm^2 are obtained for trap B at 189 K and trap I at 106 K, respectively. (Trap I was observed in indium doped materialwith a trap energy of 0.22 eV). These values are 5 to 7 orders of magnitude smaller than the extrapolated values obtained from the detailed balance principle for the capture cross-section.

Table 8 Experimentally determined trap parameters in Au/ZnSe Schottky barriers

Trap	E_t (eV)	σ_∞ exp (α/k) (cm^2)	T range (K)
A	0.33	2×10^{-13}	155-175
B	0.35	3×10^{-14}	185-215
C	0.42	8×10^{-17}	285-350
D	0.71	2×10^{-14}	360-400
E	0.86	1×10^{-13}	380-440

The difference may be in part explained by taking into account the temperature dependence of the capture cross-section. For the aforementioned traps, an exponential dependence of the capture cross-section with reciprocal temperature is observed. From the slope of a ln τ_c versus 1/T plot, apparent activation energies ΔE_B for capture of electrons of 0.10, 0.12 and 0.05 eV are calculated for traps A, B, and I respectively. Assuming that the activation process of the capture cross section is valid over the entire range of measurement, a value of σ_∞ may be obtained according to eq. (12):

$$\sigma_n = \sigma_\infty \exp\ (\Delta E_B/kT) \qquad (12)$$

where σ_n is the value obtained from Eq. (11). For the traps I, A and B, the calculated values of σ_∞ are respectively 1.0×10^{-16} cm^2, 3.8×10^{-16} cm^2 and 1.5×10^{-15} cm^2, in fair agreement with the values reported in Table 8 for the capture cross-section prefactor. One possible explanation for the larger values of the prefactor calculated by detailed balance considerations is that the electric field strongly enhances the thermal emission rates in the space-charge region.

To further elucidate the nature of the defects that were observed, the effect of excess zinc partial pressure present during growth on defect concentrations were investigated. It was observed that different growth and doping conditions of the epitaxial layer influenced the presence and concentration of the different traps. The two high temperature traps (D and E) were not observed in the ZnSe/GaAs heterojunctions, suggesting that they are associated with the gold-zinc selenide interface. This is illustrated in Fig. 5, where trap concentrations in the layer are plotted against the

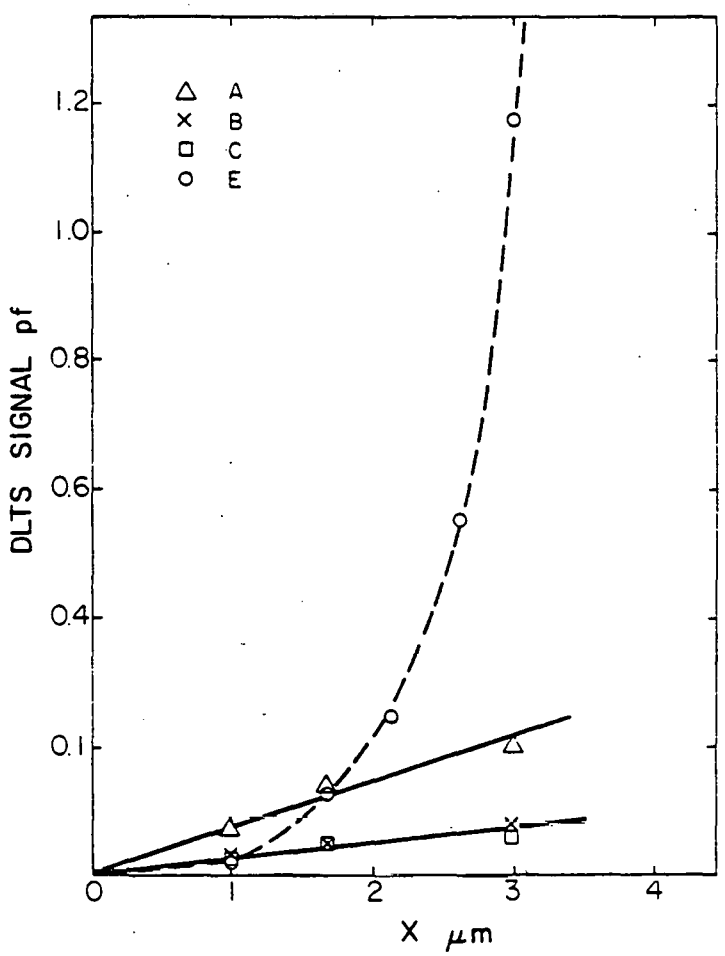

Fig. (5) Trap concentration profile in Au/ZnSe

distance from the gold-zinc selenide interface. Traps A, B and C have a constant concentration through the layer while trap E is concentrated at the gold-zinc selenide interface. Trap G in ZnSe/GaAs heterojunctions and trap C in Au/ZnSe Schottky diodes appear almost at the same temperature range, but their measured activation energy and capture cross-section are different. This suggests that trap G could be related to the zinc selenide-gallium arsenide interface (or could be a hole trap in the GaAs side of the heterojunction) while trap C is present in constant concentration through ZnSe epitaxial layer, as illustrated in Fig. 5.

Trap D, on the other hand, which is not seen in all samples has a concentration ten times smaller than trap E. Therefore trap D could be due to some residual impurities incorporated during the growth. Trap I was present in the ZnSe/GaAs heterojunction as well as in the Au/ZnSe Schottky diodes obtained with indium doped ZnSe layers. However it was not present in Schottky diodes made on undoped material. This suggests that trap I is related to a group III impurity. In the heterojunction gallium diffusing from the substrate at the zinc-selenide-gallium arsenide interface could be the impurity source. While the indium dopant in the bulk of the epitaxial layer could be the source in the indium doped ZnSe film.

Traps A and B are the deep levels that are common to all the diodes studied. Their relative concentration however may vary widely depending upon the growth conditions. This can be seen in Fig.6 , where the trap concentration variation with zinc/selenium ratio is reported. The slope on the log-log plot is +1 for traps B and E and +2 for trap A. Thus concentration dependence on zinc pressure can be described by:

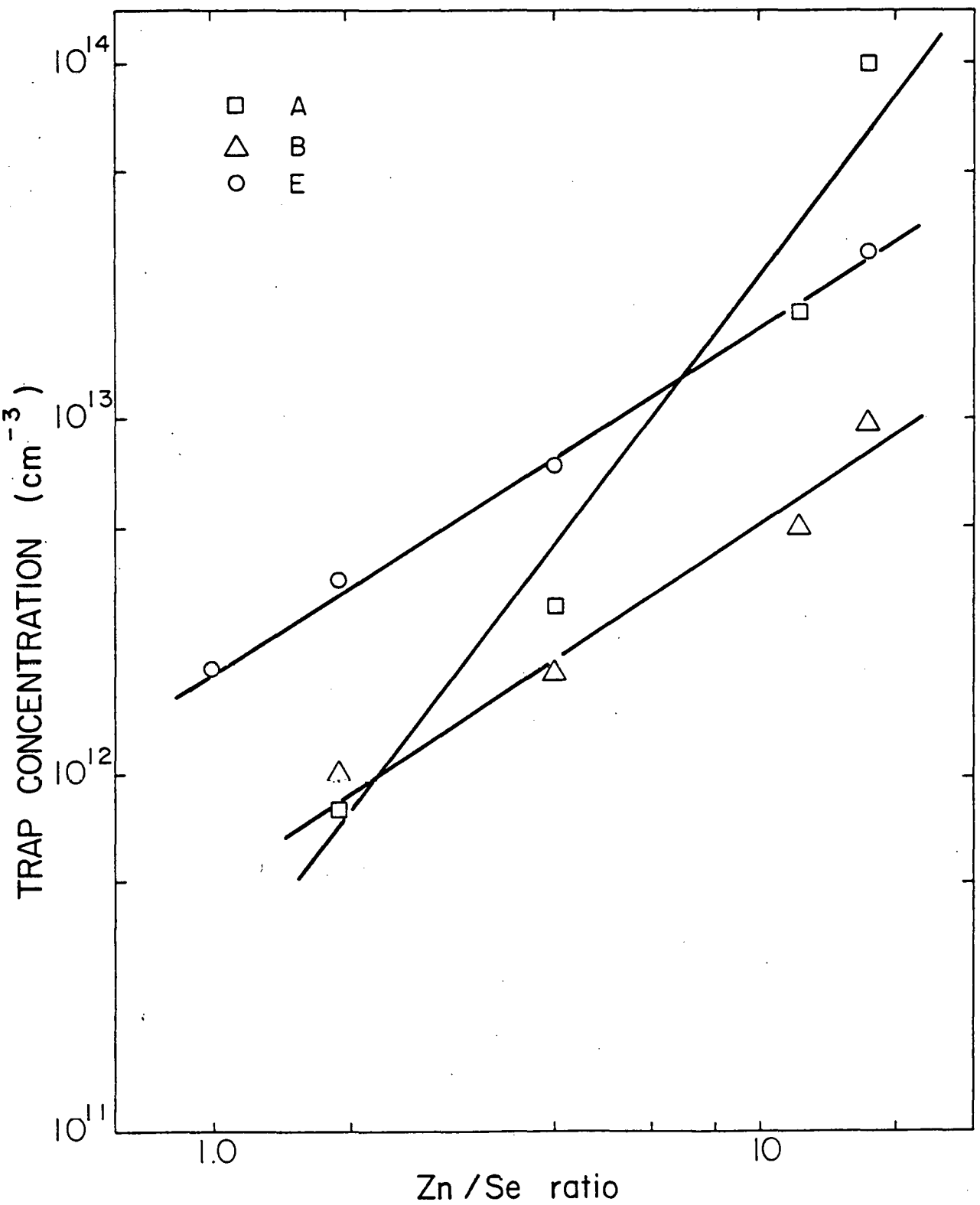

Fig. 6 Deep level trap concentration vs. Zn/Se ratio in gas phase.

$$N_T = KP_{Zn}^{n} \tag{13}$$

where n is the slope obtain from the log N_T vs P_{Zn} plot. The stronger dependence of trap A on the excess zinc partial pressure suggests that it must involve a donor whose nature itself is related to [Zn]/[Se] stoichiometry ratio.

From the dependence of trap concentration on zinc pressure, the nature of the traps can be elucidated provided equilibrium is maintained during growth, For example, the equilibrium of selenium vacancies and the vapor phase can be described by:

$$Zn(g) \rightarrow Zn_{Zn}^{x} + V_{Se}^{x} \tag{14}$$

The selenium vacancy concentration V_{Se}^{x} is equal to

$$\left[V_{Se}^{x}\right] = K_{Se} P_{Zn}^{1} \tag{15}$$

This incorporation law shows that the concentration of neutral selenium vacancies increases as a power of one with the zinc partial pressure. In Table 9 similar equations are reported for the Schottky disorder, the formation of selenium divacancies by pairing of selenium vacancies. The relevant ionization reaction of the vacancies and divacancies are also given.

Although the selenium vacancy concentration varies linearly with zinc pressure, the divacancy concentration varies as the square of the zinc pressure. If V_{Se}^{x} is substituted by its expression in eq. (15) the divacancy concentration becomes:

$$\left[\left(V_{Se}\right)_2^{x}\right] = K_D \, K_{Se}^{2} \, P_{Zn}^{2} \tag{16}$$

Thus from the pressure dependence of the trap concentration several conclusions may be made. Traps A, B and E are related to the selenium site. Defects such as substitutional impurities on the selenium site or selenium vacancies are important. Indeed, Yu and Park[16] ascribed a level at 0.9 eV from the

Table 9 Defect reactions for ZnSe

(a) Incorporation of zinc:	$Zn(g) \rightarrow Zn_{Zn}^{x} + V_{Se}^{x}$
	$\left[V_{Se}^{x}\right] = K_{Se}\, P_{Zn}$
(b) Schottky disorder:	$0 \rightleftarrows V_{Zn}^{x} + V_{Se}^{x}$
	$\left[V_{Se}^{x}\right] = K_{S} \left[V_{Zn}^{x}\right]^{-1}$
(c) Divacancy creation:	$2\, V_{Se}^{x} \rightarrow (V_{Se})_{2}^{x}$
	$\left[(V_{Se})_{2}^{x}\right] = K_{D} \left[V_{Se}^{x}\right]^{2}$
(d) Ionization of vacancy:	$V_{Se}^{x} \rightleftarrows V_{Se}^{\cdot} + e'$
	$n = K_{iv} \dfrac{\left[V_{Se}^{x}\right]}{\left[V_{Se}^{\cdot}\right]}$
(e) Ionization of a divacancy:	$(V_{Se})_{2}^{x} \rightarrow (V_{Se})_{2}^{\cdot\cdot} + 2e'$
	$n^{2} = K_{id} \dfrac{\left[(V_{Se})_{2}^{x}\right]}{\left[(V_{Se})_{2}^{\cdot\cdot}\right]}$

*Kroger-Vink notation

bottom of the conduction band to the selenium vacancy by measuring Arrhenius plots of resistivity in undoped ZnSe.

As for trap C, Jones and Woods observed several defects using luminescence and ascribed the impurities such as Cl, In and Ga. Presumably electron trap C could be a deep donor such as Cl_{Se}, $V_{Se}Ga_{Zn}$ or V_{Se}-In_{Zn} complexes.

Since the concentration of trap A varies as the square of the zinc pressure, this trap must presumably be related to the selenium divacancy. Finally, we may point out the fact that the total concentration of deep electron traps in the material is of the order of 10^{14} cm^{-3}, a minor part of the total donor concentration N_D-N_A is as high as 10^{17} cm^{-3}. It indicates that there are at least 10^{17} cm^{-3} shallow donors in high conductivity ZnSe, suggesting that the material can be made readily n type when the background impurity concentration is minimized.

Nevertheless the Hall mobility measurements show that the films are heavily compensated. Therefore large quantities of acceptor defects are present. Since transient capacitance spectroscopy on Schottky diodes is insensitive to minority (acceptor like) carrier traps, these defect levels have not yet been determined. In this case optically excited capacitance techniques are needed. Preliminary results using the spectral response of the photocapacitance signal on heterojunctions suggest that large quantities of acceptor like defect states are present in certain junctions.

WORK PROJECTED BETWEEN 15 MARCH AND 15 JUNE 1980

1. The growth and characterization of ZnSSe films prepared under zinc excess conditions will begin after the CVD apparatus is modified.
2. Hall measurements on high conductivity ZnSSe epitaxially grown on p-type GaAs will be performed.
3. Deep level transient capacitance spectroscopy measurements will be performed on deliberately doped ZnSSe.
4. The optical cryostat system will be completed.

EFFORT DEVOTED TO THIS PROJECT

During this academic year the principal investigator has spent 10% of his time on this project; summer effort was 100% of the time for one and one-half months. The 10% time effort will be continued until 15 June 1981. Three full time graduate research assistants have been associated with this project, Mr. Paul Besomi, Mr. Wallace Leigh and Mr. Keith Christianson Mr. Paul Besomi has been supported in part by a Northwestern fellowship during this last year. Mr. Besomi will be graduating by June, 1981. It is intended that Keith Christianson and Wallace Leigh continue on this contract.

PUBLICATIONS

P. Besomi and B.W. Wessels, Deep level defects in Au/ZnSe Schottky Diodes, Electronic Lett. 16, 794 (1980).

P. Besomi and B. W. Wessels, High conductivity heteroepitaxial ZnSe films, Appl. Phys. Lett 37, 955 (1980).

P. Besomi and B.W. Wessels, Growth and characterization of heteroepitaxial zinc selenide, submitted for publication.

PRESENTATIONS

Growth and Characterization of Heteroepitaxial Zinc Selenide, Electronic Materials Conference - AIME, Ithaca, N.Y. June 26, 1980.

Deep Level Defects in Au/ZnSe Schottky Diodes, Electrochemical Society, Hollywood, Florida, Oct. 6-9, 1980.

REFERENCES

1. M. Aven and H. H. Woodbury, Appl. Phys. Lett., 1, 53 (1962).

2. T. Yao, Y. Makita and S. Maekawa, Appl. Phys. Lett., 35, 97 (1979).

3. R. K. Swank, M. Aven and J. A. Devine, J. Appl. Phys. 40, 89 (1969).

4. A. M. Cowley, J. Appl. Phys. 37, 3024 (1966).

5. W. M. Yim and E. J. Stofko, J. Electrochem. Soc. 119, 381 (1972).

6. J. L. Merz, H. Kukimoto, K. Nassau and J. W. Shiever, Phys. Rev. B6, 545 (1972).

7. A. Yoshikawa and Y. Sakai, Jpn. J. Appl. Phys. 14, 1547 (1975).

8. D. Franzosi, C. Ghezzi and E. Gambia, Appl. Phys. 21, 83 (1980).

9. G. E. Stillman and C. M. Wolfe, Thin Solid Films 37, 69 (1976).

10. B. R. Sethi, D. C. Mathur and J. Woods, J. Appl. Phys. 49, 3618 (1978).

11. G. Jones and J. Woods, J. Phys. D9, 799 (1976).

12. M. Aven, J. Appl. Phys. 42, 1204 (1971).

13. D. V. Lang, J. Appl. Phys. 45, 3023 (1974).

14. P. Besomi and B. Wessels, J. Appl. Phys. 51, 4305 (1980).

15. C. Grill, B. Gastide, G. Sagnes and M. Rouzeyre, J. Appl. Phys. 50, 1375 (1979).

16. P. W. Yu and Y. S. Park, Appl. Phys. Lett. 22, pp. 345-347 (1974).

17. G.Jones and J. Woods, J. Lumin. 9, 389 (1974).